

Potential synergistic effects of sorafenib and CP-31398 for treating anaplastic thyroid cancer with p53 mutations

JIIN-TORNG WU^{1*}, CHING-LING LIN^{2,3*}, CHI-JUNG HUANG^{4,6}, YU-CHE CHENG^{4,6,7},
CHIH-CHENG CHIEN^{6,8} and YUNG-CHUAN SUNG^{6,9}

Divisions of ¹Respiratory Therapy and Chest Medicine, and ²Endocrinology and Metabolism, Department of Internal Medicine, Cathay General Hospital; ³Department of Internal Medicine, School of Medicine, College of Medicine, Taipei Medical University, Taipei 11031; ⁴Department of Medical Research, Cathay General Hospital; ⁵Department of Biochemistry, National Defense Medical Center, Taipei 11490; ⁶School of Medicine, College of Medicine, Fu Jen Catholic University, New Taipei 24205; ⁷Institute of Biomedical Engineering, Center for Biocellular Engineering, National Central University, Taoyuan 32001; ⁸Department of Anesthesiology, Cathay General Hospital; ⁹Division of Hematology/Oncology, Department of Internal Medicine, Cathay General Hospital, Taipei 10630, Taiwan, R.O.C.

Received July 10, 2019; Accepted December 19, 2019

DOI: 10.3892/ol.2020.11377

Abstract. Thyroid cancer is the most commonly diagnosed endocrine cancer. Anaplastic thyroid cancer (ATC) is the most aggressive type of thyroid cancer and has a poor prognosis. Loss of p53 function has been reported to lead to poorly differentiated thyroid tumors; therefore, mutant p53 protein can be considered a crucial therapeutic target in patients with ATC. Sorafenib, a multi-kinase inhibitor, has been approved for the treatment of metastatic and differentiated thyroid cancer. Combined targeted therapy, including sorafenib, may be clinically significant for patients with ATC harboring p53 mutations. In the present study, CP-31398, a p53-restoring agent, was used to improve the therapeutic efficacy of sorafenib in SW579 cells, an ATC cell line harboring p53 mutations. The molecular function of CP-31398 was evaluated using western blot analysis and a luciferase reporter assay. The decreased viability of SW579 cells, following CP-31398 treatment, was augmented by sorafenib, and CP-31398 enhanced the antimitogenic effect of sorafenib; thus, sorafenib and CP-31398 synergistically inhibited the growth of SW579 cells. These results indicate

a potential clinical application of CP-31398 for patients with ATC harboring p53 abnormalities, since these individuals generally respond poorly to sorafenib alone.

Introduction

Thyroid cancer is the most commonly diagnosed endocrine cancer with ~60,000 new cases diagnosed in the USA in 2018 (1,2). Thyroid cancer is not restricted to a certain age group; however, its aggressiveness increases significantly with the age of the patient (2). Anaplastic thyroid cancer (ATC) is the most aggressive type of thyroid cancer. The incidence rate of ATC has increased between 1973 and 2014, and is still associated with a higher risk of tumor progression and cancer metastasis (3).

Normal p53 acts as a tumor suppressor gene that contributes to the prevention of tumor growth (4). However, mutant p53 proteins may acquire oncogenic properties that promote tumor invasion, metastasis, cancer cell proliferation and survival (5). Point mutations in p53 are frequently detected in 50-80% of ATC tissues (6). Loss of p53 function has been reported to result in poorly differentiated thyroid tumors (6). Hence, mutant p53 protein can be considered a crucial therapeutic target in patients with ATC (6-8).

Several tyrosine kinase inhibitors (TKIs) have been used to treat advanced thyroid cancer, due to their ability to block kinases or kinase receptors (9,10). TKIs can either repress cell proliferation or attenuate the neoplastic transformation of thyroid cells (11). For example, sorafenib, a multi-kinase inhibitor that acts predominantly through the inhibition of Raf-kinase and vascular endothelial growth factor receptor 2, has been approved for the treatment of metastatic and differentiated thyroid cancer (12,13). However, although sorafenib may be effective in the treatment of advanced medullary thyroid cancer, it is not effective against ATC with a poor survival rate (14,15). Combination treatments might improve outcomes in ATC (15), which emphasizes that combined

Correspondence to: Dr Yung-Chuan Sung, Division of Hematology/Oncology, Department of Internal Medicine, Cathay General Hospital, Sec. 4, 280 Renai Road, Taipei 10630, Taiwan, R.O.C.
E-mail: yungchuans@cgh.org.tw

*Contributed equally

Abbreviations: ATC, anaplastic thyroid cancer; TKIs, tyrosine kinase inhibitors

Key words: ATC, p53 mutation, sorafenib, CP-31398, combined targeted therapy

targeted therapy may be highly effective for advanced thyroid carcinomas (16).

A large number of drug candidates, including small molecules or chemotherapeutic agents, have been identified or designed to rescue mutant *p53* and reactivate its antitumor capacity through various mechanisms. For example, PRIMA-1 can restore active conformation of mutant *p53* and PK7088 can upregulate *p21* expression and apoptotic functions (7,17). In the present study, CP-31398, a stabilizing agent that restores the wild-type conformation of mutated *p53* protein (18), was used to improve the chemotherapeutic efficacy of sorafenib for *p53*-mutated ATC cells. The molecular function of CP-31398 was evaluated using western blot analysis and a luciferase reporter assay. Sorafenib and CP-31398 synergistically inhibited the viability of the SW579 ATC cell line. Furthermore, it was demonstrated that the combination of targeted therapy (with sorafenib) and CP-31398 potentially changed the characteristics of *p53*-mutant ATC cells.

Materials and methods

Cell cultures. SW579 cells that harbor *p53* mutations were purchased from the American Type Culture Collection. The cells were cultured in Dulbecco's modified Eagle's medium (Lonza Group, Ltd.) supplemented with 10% fetal bovine serum (Greiner Bio-One International GmbH) and antibiotics (100 U/ml penicillin and 100 µg/ml streptomycin; Lonza Group, Ltd.) at 37°C and 5% CO₂ in a humidified atmosphere.

Western blot analysis. SW579 cells were seeded onto a 15-cm dish (at a density of 3.5x10⁶) and treated with 0, 0.3 or 3 µM CP-31398 (cat. no. PZ0115; Merck KGaA) for 24 h and placed at 37°C in a humidified incubator containing 5% CO₂. Total cell lysates were prepared using radioimmunoprecipitation assay buffer (cat. no. R0278; Merck KGaA) and protease inhibitors (cat. no. P8340; Merck KGaA) on ice for 5 min. The protein concentration was determined using the Bio-Rad protein assay (Bio-Rad Laboratories, Inc.). Proteins (30 µg) were separated on NuPAGE 4-12% Bis-Tris Gel (Thermo Fisher Scientific, Inc.) and transferred to polyvinylidene difluoride membranes (cat. no. IPVH00010; Merck KGaA). The membranes were incubated with primary antibodies at room temperature for 30 min for the following proteins: *p21* (1:200; cat. no. 2947; Cell Signaling Technology, Inc.), *Noxa* (1:100; cat. no. ab13654; Abcam), *p53* (1:200; cat. no. SC-126; Santa Cruz Biotechnology, Inc.) and glyceraldehyde 3-phosphate dehydrogenase (GAPDH; 1:6,000; cat. no. AM4300; Thermo Fisher Scientific, Inc.). The membranes were subsequently incubated with secondary antibody at room temperature for 30 min. The secondary antibodies were: Biotinylated anti-rabbit IgG (1:1,000; cat. no. BA-1000; Vector Laboratories, Inc.; Maravai LifeSciences) for *p21*; biotinylated anti-mouse IgG (1:1,000; cat. no. BA-2000; Vector Laboratories, Inc.; Maravai LifeSciences) for *Noxa* and *p53*; and horseradish peroxidase-conjugated anti-mouse IgG for GAPDH (1:5,000; cat. no. ab6808; Abcam). The bands were then visualized using Vectastain ABC-Amp Chemiluminescence Detection kit (cat. no. AK-6601; Vector Laboratories, Inc.; Maravai LifeSciences) for *p21*, *Noxa* and *p53*; and the Western Lightning Ultra-ECL (cat. no. NEL113001EA; PerkinElmer, Inc.) for GAPDH; both

according to the manufacturer's instructions. Finally, images were acquired and protein bands were quantified by densitometric analysis using an Alpha Innotech FluorChem FC2 Imager (version 3.2.2; ProteinSimple). The relative protein levels were calculated and determined by normalizing their expression to that of the GAPDH internal control.

Change in viability of SW579 cells following CP-31398 treatment. The growth of SW579 cells was evaluated using MTT assay (cat. no. M5655; Merck KGaA). Firstly, SW579 cells were cultured at 1x10⁴ cells/well in 96-well plates for 24 h. To calculate the half-maximal inhibitory concentration (IC₅₀) of CP-31398, the chemosensitivity of cells was determined following incubation for 24 h at 0, 1, 1.5, 2, 2.5, 3, 3.5 and 4 µM. To evaluate the efficiency of adjuvant therapy, SW579 cells were treated with 1 µM sorafenib (cat. no. 284461-73-0; ApexBio Technology) and 3 µM CP-31398 alone or combined for 72 h and cell viability was calculated using MTT assay. The cells were then treated with 10 µl of the MTT reagent, and incubated in the dark for 4 h. Dimethyl sulfoxide (100 µl) was subsequently added to dissolve the purple precipitate formed by the viable cells. The absorbance of each well at 540 nm was read by a Synergy HT Multi-Mode microplate reader (BioTek Instruments, Inc.). Data were obtained from three independent experiments.

Cell cycle analysis through image cytometry. The cell cycle analysis of SW579 cells was performed using a fluorescence image cytometer (NucleoCounter NC-3000; ChemoMetec A/S). SW579 cells were seeded in a 10-cm dish at a density of 1.1x10⁶ cells per dish. Treatment with CP-31398, at concentrations of 0, 0.3 or 3 µM, was initiated 16 h following seeding. After a 72-h incubation, cells were harvested by trypsinization, loaded into a Via-1-Cassette (ChemoMetec), and counted according to the manufacturer's instructions. Approximately 1.5x10⁶ cells were suspended in 0.5 ml of phosphate-buffered saline (PBS), and fixed with 4.5 ml of 70% cold ethanol for at least 2 h. Subsequently, ethanol was removed, and the cells were resuspended in PBS. Cell pellets were harvested by centrifugation at 500 x g for 5 min at 4°C and incubated with 0.5 ml DAPI solution [0.1% Triton X-100 and 4',6-diamidino-2-phenylindole (DAPI)] for 5 min at 37°C. The stained cells were loaded into an NC-Slide A8 (ChemoMetec) and evaluated using a Fixed Cell Cycle-DAPI/DNA fragmentation assay protocol in the NucleoCounter NC-3000 image cytometer (ChemoMetec) (19). The acquired DNA content histograms were used to distinguish cells at different stages of the cell cycle with the NucleoView NC-3000 software (version 2.1.25.12; ChemoMetec).

Luciferase reporter assay. The *p53*-dependent reporter plasmid, PG13-luc, which carries the firefly luciferase gene driven by a promoter containing 13 *p53*-binding elements, was provided by Dr Shih-Ming Huang (Department and Graduate Institute of Biochemistry, National Defense Medical Center, Taiwan). Clones of SW579 cells expressing luciferase were obtained after transfecting the cells with PG13-luc, using the T-Pro NTRIII transfection reagent (Jifeng Biotechnology) for 5 h according to the manufacturer's protocol. The background levels of relative luciferase

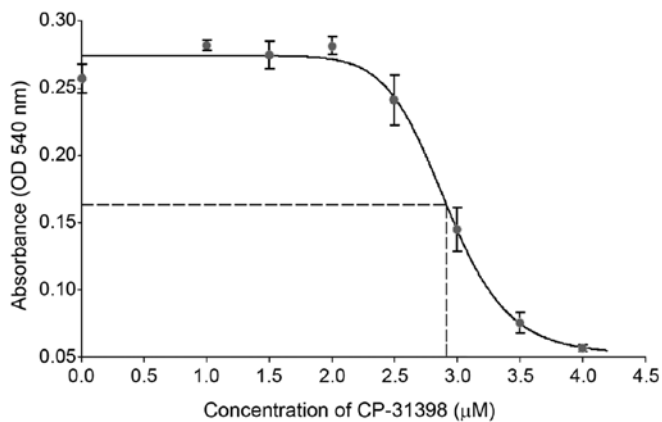


Figure 1. Potential inhibitory effect of CP-31398 on anaplastic thyroid cancer cells. SW579 cells were treated with CP-31398 (0-4.0 μ M) for 24 h. MTT reagent (10 μ l) was administered to each well, and absorbance measurements were performed at 540 nm. Data are presented in triplicate per drug concentration. The dash lines indicate the IC_{50} value (~ 3 μ M).

units (RLUs) were detected from SW579 cells without PG13-luc plasmid. Luciferase activity was measured 24 h after the cells were treated with or without CP-31398 (3 μ M). The SW579/PG13-luc cell lysate (5 μ g in 20 μ l) was added to 100 μ l of the luciferase assay reagent (Luciferase Assay System with Reporter Lysis Buffer; Promega Corporation) in white clear-bottomed 96-well plates (Greiner Bio-One International GmbH), in duplicate or triplicate for each experimental condition. Bioluminescence produced for 10 sec was automatically measured under the Centro LB 960 Microplate Luminometer (Berthold Technologies GmbH).

Statistical analysis. Statistical analysis was performed using the SPSS software (version 13.0; SPSS Inc.). Numerical data are expressed as mean \pm standard deviation. The Student's t-test was used for the analysis of two groups, and one-way analysis of variance with least significant difference for multiple comparisons was performed for determining the significance of differences between the various experimental groups. $P < 0.05$ was considered to indicate a statistically significant difference.

Results

Determination of the IC_{50} of CP-31398 in *p53*-mutated ATC cells. CP-31398 inhibited the growth of SW579 thyroid cancer cells, an ATC cell line harboring *p53* mutations (20,21). The IC_{50} of CP-31398 in SW579 cells was determined 24 h after treatment with doses ranging from 0-4 μ M. The potential inhibitory effect of CP-31398 on SW579 cells is shown in Fig. 1. The concentration of 3 μ M was chosen for the following experiments since it was closed to the IC_{50} (~ 2.9 μ M). Recent studies reported that CP-31398 restores the function of *p53* and could be considered as a therapeutic strategy for *p53*-dysfunctional cancers, including cervical cancer or esophageal cancer (22,23). The present study demonstrated that CP-31398 restored the function of mutated *p53* in SW579 cells. Firstly, 3 μ M CP-31398 induced the promoter activity of the plasmid PG13-luc that requires wild-type *p53* binding sites. As shown in Fig. 2,

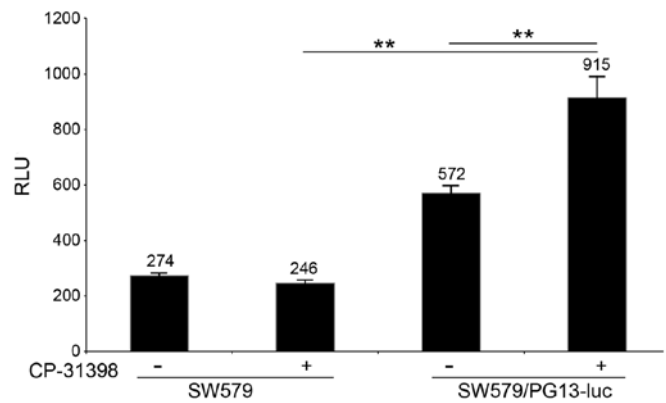


Figure 2. Restoration of *p53* activity in SW579 cells by CP-31398. SW579 cells were transfected with the pPG13-luc and/or treated with CP31398, as indicated. The luciferase activity was measured 24 h after transfection. Data (means \pm standard deviation) are presented as RLUs of triplicate wells and indicated on top of the bars. The data were analyzed using one-way analysis of variance followed by least significant difference post hoc test. ** $P < 0.01$. +, cells with CP-31398 treatment; -, cells without CP-31398 treatment; RLUs, relative luciferase units.

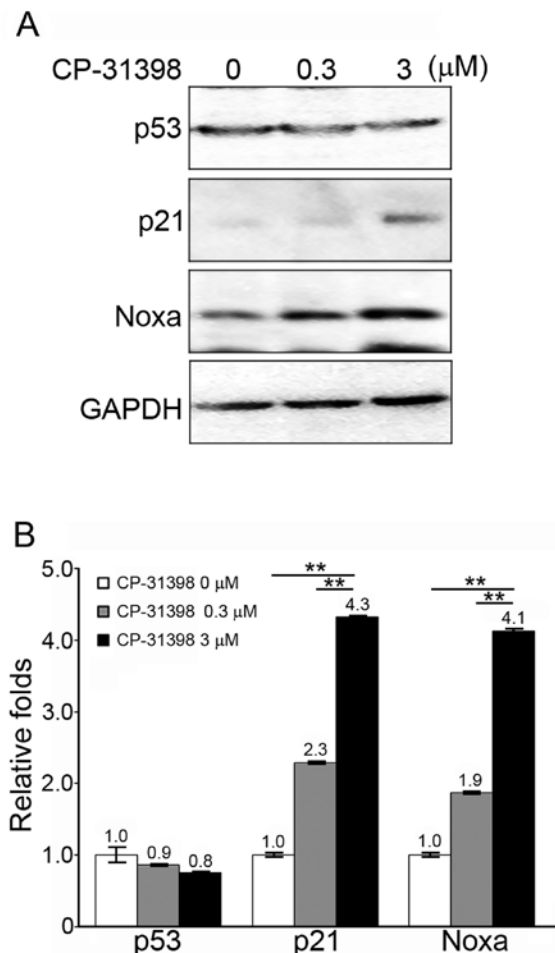


Figure 3. Western blot analyses of SW579 cells treated with CP-31398. SW579 cells were incubated with 0, 0.3 or 3 μ M CP-31398 for 24 h. (A) Protein levels of *p53*, *p21* and *Noxa*. (B) Relative quantification of *p53*, *p21* and *Noxa* from western blotting. Aliquots of 30 μ g of lysate were separated by NuPAGE Bis-Tris gels and transferred to membranes. Images were acquired and quantified using an Alpha Innotech FluorChem FC2 Imager. GAPDH was used as endogenous control. Results were representative of one of 2-to-3 independent experiments with similar results. Data were expressed as the means \pm standard deviation. Student's t-test was used. ** $P < 0.01$.

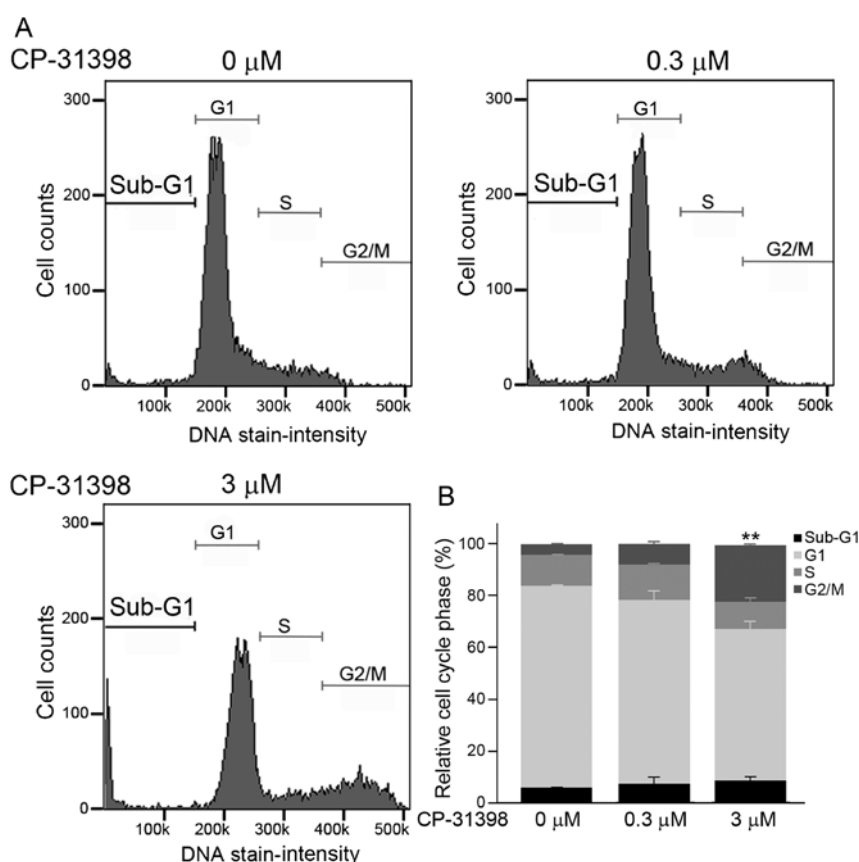


Figure 4. Effects of CP-31398 on the number of SW579 cells in the cell cycle. (A) Cell cycle distribution. (B) Statistical analysis of cell cycle phases. SW579 cells were incubated with 0, 0.3 or 3 μ M CP-31398 for 72 h. The CP-31398-treated cells were loaded into a Via-1-Cassette and analyzed for DAPI dyes, using a fluorescence image cytometer (NucleoCounter NC-3000). Data were expressed as the means \pm standard deviation. Student's t-test was used. ** $P < 0.01$.

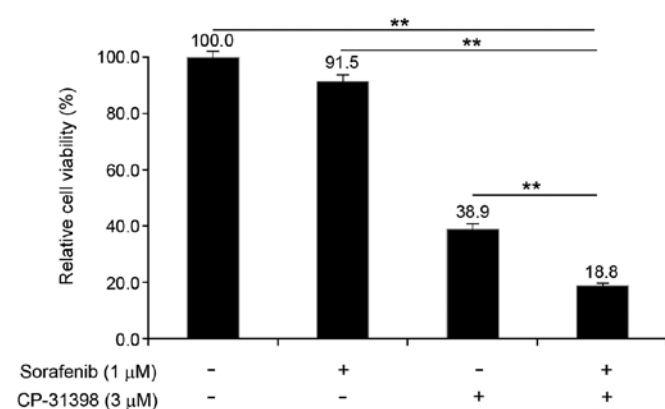


Figure 5. Suppression of SW579 cell viability by sorafenib and CP-31398 combination treatment. SW579 cells were treated with 1 μ M sorafenib and 3 μ M CP-31398 alone or combined for 72 h. The viability of SW579 cells (%), relative to cells with no drug treatment) was evaluated using the MTT assay. Data (mean \pm standard deviation) from 4-6 independent repeats are presented. The data was analyzed using one-way analysis of variance, followed by least significant difference post hoc test. ** $P < 0.01$. +, cells with sorafenib or CP-31398 treatment; -, cells without sorafenib or CP-31398 treatment.

CP-31398 significantly increased the luciferase activity from 572 ± 26 RLUs in non-treated cells to 915 ± 76 RLUs in treated SW579/PG13-luc cells ($P < 0.01$). Secondly, SW579 cells treated with CP-31398 (3 μ M) exhibited significantly increased protein levels of p21 and Noxa, which are p53-dependent proteins (Fig. 3A and B).

CP-31398 induces apoptosis and G2/M cell cycle arrest in SW579 cells. To determine whether the increased expression of p21 and Noxa in SW579 cells, following treatment with CP-31398, matched with the induction of apoptosis, the percentages of cells at each stage of the cell cycle were determined. The cell cycle distribution in SW579 cells was examined after treatment with CP-31398 at 0, 0.3 or 3 μ M for 72 h. Treatment with 3 μ M CP-31398 resulted in changes in cell cycle phases (Fig. 4A). Results from Fig. 4B demonstrated an increased percentage of cells with sub-G1 DNA content (0 to 0.3 μ M, +1.5%; 0.3 to 3 μ M, +1.0%), a decreased percentage of cells at G1 phase (0 to 0.3 μ M, -7.5%; 0.3 to 3 μ M, -12.5%), and arrested cell cycle at the G2/M phase with statistical significance (0 to 3 μ M, +3.5%; 0.3 to 3 μ M, +13.5%; $P < 0.01$).

Adjuvant therapy with sorafenib for thyroid cancer in the presence of CP-31398. Sorafenib has been used to treat different types of thyroid cancer (14,24). However, previous studies indicated that sorafenib has an IC_{50} value of 1.7 ± 0.2 μ M against SW579 cells (25). In the present study, 1 μ M sorafenib did not effectively inhibit the viability of SW579 cells, however treatment with 3 μ M CP-31398 inhibited their viability after 72 h incubation (Fig. 5). Notably, combination treatment with 1 μ M sorafenib and 3 μ M CP-31398 for 72 h resulted in a significantly greater decrease in cell viability (18.8 ± 0.9 of untreated control cells; $P < 0.01$) compared with single-agent treatments (1 μ M sorafenib, 91.5 ± 2.4 ; 3 μ M CP-31398, 38.9 ± 1.8 ; both $P < 0.01$).

Discussion

Although rare, ATC is one of the most aggressive human malignancies, and most patients with ATC have a poor prognosis, with a rate of thyroid cancer-associated mortality of almost 50% (26). In addition, Liu *et al* also reported that the 2-year overall survival rate of patients with ATC was low (26.0%) in Asia (27). In clinical settings, sorafenib provides sufficient tumor reduction to allow for thyroidectomy and radioactive iodine therapy in most types of thyroid cancer (12,28). However, Ito *et al* (14) reported that sorafenib appeared to be effective in the treatment of advanced medullary thyroid carcinoma but not ATC. Therefore, targeted therapy with sorafenib in combination with other drugs could be clinically effective for patients with ATC (15).

In the present study, SW579 cells (carrying *p53* mutations) were treated with a small-molecule agent CP-31398, which induces the desired phenotypic change (apoptosis and proliferation inhibition) in cancer cells with *p53* mutations (29,30). CP-31398 caused notably decreased viability of SW579 cells (31). Mutated *p53* (mutations at codons 151, 152, 248 and 255) is frequently detected in endocrine tumors, including ATC (21), and the DNA-binding domain of *p53* in SW579 cells was defective due to a point mutation at codon 255 (Ile to Ser) (31). In general, the DNA-binding ability and molecular function of *p53* in SW579 cells improved when they were treated with CP-31398 (31). Xu *et al* (32) reported that CP-31398 treatment stabilizes the levels of mutant *p53* and enhances p21 protein level in rhabdomyosarcoma. In the present study, the plasmid, PG13-luc, containing a *p53*-binding site in its promoter was reactivated following treatment with CP-31398 in SW579 cells. Secondly the protein expression levels of two *p53*-dependent proteins, p21 and Noxa, were increased. However, the level of mutant *p53* did not increase in the CP-31398-treated SW579 cells. These data demonstrated that the molecular function of *p53* was restored when SW579 cells were treated with the optimal concentration (3 μ M) of CP-31398. It was hypothesized that the increased levels of p21 and Noxa contributed to the reduction in cell viability, by causing cells to arrest at the G2/M phase and inducing apoptosis (33,34).

Furthermore, the present study demonstrated the reduction in the viability of SW579 cells by CP-31398 treatment to be augmented by the addition of the targeted therapeutic agent sorafenib. Nevertheless, the antitumor activity of combined targeted therapy with sorafenib and CP-31398 must be further investigated using an *in vivo* xenograft model or a real-time image of orthotopic model (35,36).

In summary, the present study demonstrated that CP-31398 induces apoptosis and arrests the cell cycle at the G2/M phase in SW579 cells, by restoring the molecular function of *p53*. Notably, CP-31398 increased the antimetastatic effect of sorafenib, and the combination of these two agents synergistically reduced the viability of SW579 cells. Overall, the present study indicates a potential clinical application of CP-31398 for treating patients with ATC harboring *p53* mutations, who generally respond poorly to sorafenib-only treatment.

Acknowledgements

The authors would like to thank Dr Shih-Ming Huang (Department of Biochemistry, National Defense Medical Center, Taipei, Taiwan R.O.C) for providing the plasmid.

Funding

The present study was supported by the Cathay General Hospital (Taipei, Taiwan; grant. no. CGH-MR-A10809; awarded to YS).

Availability of data and materials

The datasets used and/or analyzed during the current study are available from the corresponding author on reasonable request.

Authors' contributions

CLL, JTW and YCS designed the study. CLL, JTW and CJH wrote the initial version of the manuscript. CJH and CCC conducted the cell studies. CCC performed the statistical analyses. YCC performed western blotting. All authors discussed, modified and approved the final version of the manuscript.

Ethics approval and consent to participate

Not applicable.

Patient consent for publication

Not applicable.

Competing interests

The authors declare that they have no competing interests.

References

1. Siegel RL, Miller KD and Jemal A: Cancer statistics, 2018. *CA Cancer J Clin* 68: 7-30, 2018.
2. Blackburn BE, Ganz PA, Rowe K, Snyder J, Wan Y, Deshmukh V, Newman M, Fraser A, Smith K, Herget K, *et al*: Aging-related disease risks among young thyroid cancer survivors. *Cancer Epidemiol Biomarkers Prev* 26: 1695-1704, 2017.
3. Janz TA, Neskey DM, Nguyen SA and Lentsch EJ: Is the incidence of anaplastic thyroid cancer increasing: A population based epidemiology study. *World J Otorhinolaryngol Head Neck Surg* 5: 34-40, 2018.
4. Labuschagne CF, Zani F and Vousden KH: Control of metabolism by *p53*-cancer and beyond. *Biochim Biophys Acta Rev Cancer* 1870: 32-42, 2018.
5. Muller PA and Vousden KH: *p53* mutations in cancer. *Nat Cell Biol* 15: 2-8, 2013.
6. Manzella L, Stella S, Pennisi MS, Tirro E, Massimino M, Romano C, Puma A, Tavarelli M and Vigneri P: New insights in thyroid cancer and *p53* family proteins. *Int J Mol Sci* 18: E1325, 2017.
7. Li Y, Wang Z, Chen Y, Petersen RB, Zheng L and Huang K: Salvation of the fallen angel: Reactivating mutant *p53*. *Br J Pharmacol* 176: 817-831, 2019.
8. Liu L, Li D, Chen Z, Yang J, Ma Y, Cai H, Shan C, Lv Z and Zhang X: Wild-type *p53* induces sodium/iodide symporter expression allowing radioiodide therapy in anaplastic thyroid cancer. *Cell Physiol Biochem* 43: 905-914, 2017.
9. Date E, Okamoto K, Fumita S and Kaneda H: Gastrointestinal perforation related to lenvatinib, an anti-angiogenic inhibitor that targets multiple receptor tyrosine kinases, in a patient with metastatic thyroid cancer. *Invest New Drugs* 36: 350-353, 2018.
10. Saito Y, Sugino K, Takami H, Matsuzaki K, Urano T, Ohkuwa K, Kitagawa W, Nagahama M, Kawakubo H, Ito K and Kitagawa Y: Clinical status and treatment of liver metastasis of differentiated thyroid cancer using tyrosine kinase inhibitors. *World J Surg* 42: 3632-3637, 2018.
11. Cabanillas ME, McFadden DG and Durante C: Thyroid cancer. *Lancet* 388: 2783-2795, 2016.

12. Corrado A, Ferrari SM, Politti U, Mazzi V, Miccoli M, Materazzi G, Antonelli A, Ullisse S, Fallahi P and Miccoli P: Aggressive thyroid cancer: Targeted therapy with sorafenib. *Minerva Endocrinol* 42: 64-76, 2017.
13. Ramakrishnan V, Timm M, Haug JL, Kimlinger TK, Wellik LE, Witzig TE, Rajkumar SV, Adjei AA and Kumar S: Sorafenib, a dual Raf kinase/vascular endothelial growth factor receptor inhibitor has significant anti-myeloma activity and synergizes with common anti-myeloma drugs. *Oncogene* 29: 1190-1202, 2010.
14. Ito Y, Onoda N, Ito KI, Sugitani I, Takahashi S, Yamaguchi I, Kabu K and Tsukada K: Sorafenib in Japanese patients with locally advanced or metastatic medullary thyroid carcinoma and anaplastic thyroid carcinoma. *Thyroid* 27: 1142-1148, 2017.
15. Chen G, Nicula D, Renko K and Derwahl M: Synergistic anti-proliferative effect of metformin and sorafenib on growth of anaplastic thyroid cancer cells and their stem cells. *Oncol Rep* 33: 1994-2000, 2015.
16. Orlandi F, Caraci P, Berruti A, Puligheddu B, Pivano G, Dogliotti L and Angeli A: Chemotherapy with dacarbazine and 5-fluorouracil in advanced medullary thyroid cancer. *Ann Oncol* 5: 763-765, 1994.
17. Binayke A, Mishra S, Suman P, Das S and Chander H: Awakening the 'guardian of genome': Reactivation of mutant p53. *Cancer Chemother Pharmacol* 83: 1-15, 2019.
18. Mularski J, Malarz K, Pacholczyk M and Musiol R: The p53 stabilizing agent CP-31398 and multi-kinase inhibitors. Designing, synthesizing and screening of styrylquinazoline series. *Eur J Med Chem* 163: 610-625, 2019.
19. Beberok A, Rzepka Z, Respondek M, Rok J, Stradowski M and Wrzesniok D: Moxifloxacin as an inducer of apoptosis in melanoma cells: A study at the cellular and molecular level. *Toxicol In Vitro* 55: 75-92, 2019.
20. Huang LC, Tam KW, Liu WN, Lin CY, Hsu KW, Hsieh WS, Chi WM, Lee AW, Yang JM, Lin CL and Lee CH: CRISPR/Cas9 genome editing of epidermal growth factor receptor sufficiently abolished oncogenicity in anaplastic thyroid cancer. *Dis Markers* 2018: 3835783, 2018.
21. Yoshimoto K, Iwahana H, Fukuda A, Sano T, Saito S and Itakura M: Role of p53 mutations in endocrine tumorigenesis: Mutation detection by polymerase chain reaction-single strand conformation polymorphism. *Cancer Res* 52: 5061-5064, 1992.
22. Liu L, Yu TT, Ren CC, Yang L, Cui SH and Zhang XA: CP-31398 inhibits the progression of cervical cancer through reversing the epithelial mesenchymal transition via the downregulation of PAX2s. *J Cell Physiol* 234: 2929-2942, 2019.
23. Zhong B, Shingyoji M, Hanazono M, Nguyen TTT, Morinaga T, Tada Y, Hiroshima K, Shimada H and Tagawa M: A p53-stabilizing agent, CP-31398, induces p21 expression with increased G2/M phase through the YY1 transcription factor in esophageal carcinoma defective of the p53 pathway. *Am J Cancer Res* 9: 79-93, 2019.
24. Krajewska J, Handkiewicz-Junak D and Jarzab B: Sorafenib for the treatment of thyroid cancer: An updated review. *Expert Opin Pharmacother* 16: 573-583, 2015.
25. Wang L, Zhang Y, Zhang Q, Zhu G, Zhang Z, Duan C, Lu T and Tang W: Discovery of potent Pan-Raf inhibitors with increased solubility to overcome drug resistance. *Eur J Med Chem* 163: 243-255, 2019.
26. Salehian B, Liem SY, Mojazi Amiri H and Maghami E: Clinical trials in management of anaplastic thyroid carcinoma; progressions and set backs: A systematic review. *Int J Endocrinol Metab* 17: e67759, 2019.
27. Liu TR, Xiao ZW, Xu HN, Long Z, Wei FQ, Zhuang SM, Sun XM, Xie LE, Mu JS, Yang AK, *et al*: Treatment and prognosis of anaplastic thyroid carcinoma: A clinical study of 50 cases. *PLoS One* 11: e0164840, 2016.
28. Danilovic DLS, Castro G Jr, Roitberg FSR, Vanderlei FAB, Bonani FA, Freitas RMC, Coura-Filho GB, Camargo RY, Kulcsar MA, Marui S and Hoff AO: Potential role of sorafenib as neoadjuvant therapy in unresectable papillary thyroid cancer. *Arch Endocrinol Metab* 62: 370-375, 2018.
29. Arihara Y, Takada K, Kamihara Y, Hayasaka N, Nakamura H, Murase K, Ikeda H, Iyama S, Sato T, Miyanishi K, *et al*: Small molecule CP-31398 induces reactive oxygen species-dependent apoptosis in human multiple myeloma. *Oncotarget* 8: 65889-65899, 2017.
30. He XX, Zhang YN, Yan JW, Yan JJ, Wu Q and Song YH: CP-31398 inhibits the growth of p53-mutated liver cancer cells in vitro and in vivo. *Tumour Biol* 37: 807-815, 2016.
31. Grassi ES, Vezzoli V, Negri I, Labadi A, Fugazzola L, Vitale G and Persani L: SP600125 has a remarkable anticancer potential against undifferentiated thyroid cancer through selective action on ROCK and p53 pathways. *Oncotarget* 6: 36383-36399, 2015.
32. Xu J, Timares L, Heilpern C, Weng Z, Li C, Xu H, Pressey JG, Elmets CA, Kopelovich L and Athar M: Targeting wild-type and mutant p53 with small molecule CP-31398 blocks the growth of rhabdomyosarcoma by inducing reactive oxygen species-dependent apoptosis. *Cancer Res* 70: 6566-6576, 2010.
33. Karimian A, Ahmadi Y and Yousefi B: Multiple functions of p21 in cell cycle, apoptosis and transcriptional regulation after DNA damage. *DNA Repair (Amst)* 42: 63-71, 2016.
34. Shibue T, Takeda K, Oda E, Tanaka H, Murasawa H, Takaoka A, Morishita Y, Akira S, Taniguchi T and Tanaka N: Integral role of Noxa in p53-mediated apoptotic response. *Genes Dev* 17: 2233-2238, 2003.
35. Tran Cao HS, Kaushal S, Snyder CS, Ongkeko WM, Hoffman RM and Bouvet M: Real-time imaging of tumor progression in a fluorescent orthotopic mouse model of thyroid cancer. *Anticancer Res* 30: 4415-4422, 2010.
36. Kim S, Yazici YD, Calzada G, Wang ZY, Younes MN, Jasser SA, El-Naggar AK and Myers JN: Sorafenib inhibits the angiogenesis and growth of orthotopic anaplastic thyroid carcinoma xenografts in nude mice. *Mol Cancer Ther* 6: 1785-1792, 2007.